Redox Biology 12 (2017) 8–17

Contents lists available at ScienceDirect

Redox Biology

journal homepage: www.elsevier.com/locate/redox

Research Paper

Ablation of ferroptosis regulator glutathione peroxidase 4 in forebrain neurons promotes cognitive impairment and neurodegeneration

William Sealy Hambright[a], Rene Solano Fonseca[a], Liuji Chen[a], Ren Na[a], Qitao Ran[a,b,*]

[a] Department of Cell Systems and Anatomy, University of Texas Health Science Center, San Antonio, TX, USA
[b] Research Service, South Texas Veterans Health Care System, San Antonio, TX, USA

ARTICLE INFO

Keywords:
Ferroptosis
Neurodegeneration
Cognitive impairment
Alzheimer's disease
Glutathione peroxidase 4
Transgenic mice

ABSTRACT

Synaptic loss and neuron death are the underlying cause of neurodegenerative diseases such as Alzheimer's disease (AD); however, the modalities of cell death in those diseases remain unclear. Ferroptosis, a newly identified oxidative cell death mechanism triggered by massive lipid peroxidation, is implicated in the degeneration of neurons populations such as spinal motor neurons and midbrain neurons. Here, we investigated whether neurons in forebrain regions (cerebral cortex and hippocampus) that are severely afflicted in AD patients might be vulnerable to ferroptosis. To this end, we generated Gpx4BIKO mouse, a mouse model with conditional deletion in forebrain neurons of glutathione peroxidase 4 (Gpx4), a key regulator of ferroptosis, and showed that treatment with tamoxifen led to deletion of Gpx4 primarily in forebrain neurons of adult Gpx4BIKO mice. Starting at 12 weeks after tamoxifen treatment, Gpx4BIKO mice exhibited significant deficits in spatial learning and memory function versus Control mice as determined by the Morris water maze task. Further examinations revealed that the cognitively impaired Gpx4BIKO mice exhibited hippocampal neurodegeneration. Notably, markers associated with ferroptosis, such as elevated lipid peroxidation, ERK activation and augmented neuroinflammation, were observed in Gpx4BIKO mice. We also showed that Gpx4BIKO mice fed a diet deficient in vitamin E, a lipid soluble antioxidant with anti-ferroptosis activity, had an expedited rate of hippocampal neurodegeneration and behavior dysfunction, and that treatment with a small-molecule ferroptosis inhibitor ameliorated neurodegeneration in those mice. Taken together, our results indicate that forebrain neurons are susceptible to ferroptosis, suggesting that ferroptosis may be an important neurodegenerative mechanism in diseases such as AD.

1. Introduction

Aging is the biggest risk factor for neurodegeneration diseases such as Alzheimer's disease (AD); therefore, as the population ages, the incidence of AD increases exponentially. The underlying cause of AD is the degeneration of neuron populations important for learning and memory. The degeneration process includes the progressive degradation of synapses and eventual death of neurons. At present, the modalities of neuron death remain unclear. Because studies have detected signatures of apoptosis in post-mortem brain tissue from AD patients and showed that Aβ could induce apoptosis in neurons, it is thought that apoptosis is likely responsible for the immense neurodegeneration in AD [1,2]. However, concomitant pathological features in AD brains such as augmented inflammation and the chronic nature of the degenerating process cannot be explained by apoptotic cell death alone [3,4]. Further, drugs targeting apoptosis for the treatment of neurodegenerative diseases (e.g., caspase inhibition or MKL inhibition) have been largely ineffective in the clinic [5,6], highlighting the potential for alternative cell death modalities in neurodegeneration.

Oxidative damage is well-demonstrated in AD brains [7,8]. Because the brain is rich in lipids containing polyunsaturated fatty acids (PUFAs), lipid peroxidation is the prominent type of oxidative damage. Indeed, lipid peroxidation is believed to be an early event in AD pathogenesis [9]. Dysregulation of iron, which can augment the production of reactive oxygen species (ROS), is also evident in AD

Abbreviations: AD, Alzheimer's disease; Gpx4, glutathione peroxidase 4; TAM, tamoxifen; CC, cerebral cortex; HC, hippocampus; 4-HNE, 4-hydroxynonenol; GFAP, glial fibrillary acidic protein; Iba-1, ionized calcium-binding adapter molecule-1; Syn, synaptophysin; PSD95, postsynaptic density protein; SNAP25, synaptosome associated protein; TNF-α, tumor necrosis factor alpha; IL-6, interleukin-6; IL-1β, interleukin-1 beta; PUFA, polyunsaturated fatty acid

* Correspondence to: Department of Cell Systems and Anatomy, University of Texas Health Science Center at San Antonio, 7703 Floyd Curl Dr., San Antonio, TX 78229, United States.
E-mail address: ran@uthscsa.edu (Q. Ran).

http://dx.doi.org/10.1016/j.redox.2017.01.021
Received 11 January 2017; Received in revised form 20 January 2017; Accepted 30 January 2017
Available online 01 February 2017
2213-2317/ © 2017 Published by Elsevier B.V.
This is an open access article under the CC BY-NC-ND license (http://creativecommons.org/licenses/BY-NC-ND/4.0/).

brains [10]. Interestingly, lipid peroxidation and iron dysregulation identify a new cell death mechanism called ferroptosis, a cell death pathway that is genetically, morphologically, and biochemically distinct from apoptosis [11]. Cells dying through ferroptosis release damage-associated molecular patterns (DAMPs) and lipid metabolites that are immunogenic [12,13], and are predicted to result in elevated inflammation. In fact, inflammation is a pronounced pathological feature of AD [14], which is not a feature of apoptotic cell death. Thus, ferroptosis presents an intriguing modality of neurodegeneration in AD because of its dependence on lipid peroxidation and iron dysregulation as well as its ability to induce inflammation, all of which are signatures of AD.

Lipid peroxidation is the driving force of cell death in ferroptosis [15]. Glutathione peroxidase 4 (Gpx4) is a selenoprotein glutathione peroxidase that can detoxify hydroperoxides in membrane lipids directly, thereby reducing damage to membrane function and preventing the generation of lipid peroxidation-derived reactive products such as 4-hydroxynonenal (4-HNE) [16]. Yang et al. identified Gpx4 as a key regulator of ferroptosis in cancer cells [17]. Subsequently, it was shown that ablation of Gpx4 induces ferroptosis in cell types such as renal tubular cells and T lymphocytes [13,18]. We previously reported that conditional ablation of Gpx4 in neurons of adult mice triggers rapid degeneration of spinal motor neurons likely through ferroptosis [19]. However, because those mice succumbed to motor neuron disease so quickly, it was impossible to discern whether neuron populations important for cognition are vulnerable to ferroptosis. In this study, we sought to investigate the ferroptotic potential of neurons in the forebrain regions of hippocampus and cerebral cortex that are essential for learning and memory and are severely afflicted in AD patients. We generated a novel forebrain neuron specific, tamoxifen inducible Gpx4 knockout mouse model. Following tamoxifen treatment to ablate Gpx4, we observed cognitive impairment and hippocampal neurodegeneration in those forebrain-specific Gpx4 knockout mice. In addition, we detected several markers associated with ferroptosis in those mice. We also showed that neurodegeneration and behavior dysfunction was exacerbated by placing the animals on a diet deficient in vitamin E, a lipid soluble antioxidant with anti-ferroptosis activity. We further showed that treatment with a small-molecule ferroptosis inhibitor attenuated neurodegeneration in those mice. Our results suggest ferroptosis is a potential neurodegenerative mechanism affecting neurons important for learning and memory.

2. Materials and methods

2.1. Animals, diets, and treatments

Gpx4(f/f) mice were previously described [20]. Camk2α-CreER(T2) mice, which express a tamoxifen-activatable form of Cre recombinase in forebrain neurons under the direction of Camk2α promoter [21], were purchased from the Jackson Laboratories (Cat# 012362, Bar Harbor, ME). Gpx4(f/f) mice were bred with Camk2α-CreER(T2) mice to produce Gpx4(f/+);Camk2α-CreER(T2)$^{+/0}$ mice, which were then bred with Gpx4(f/f) mice to produce Gpx4(f/f);Camk2α-CreERT$^{+/0}$ mice, also known as Gpx4BIKO mice. Gpx4BIKO mice [Gpx4(f/f);Camk2α-CreER(T2)$^{+/0}$] were bred with Gpx4(f/f) mice to produce Gpx4BIKO mice and Gpx4(f/f) mice used in the experiments. Gpx4BIKO mice and Gpx4(f/f) littermates at 2–4 months of age were enrolled in experimental cohorts. All cohorts consisted of roughly half males and half females.

To induce Gpx4 ablation, tamoxifen (T5648, Sigma) was dissolved in corn oil (10 mg/ml) and administered by intraperitoneal (i.p.) injection to Gpx4BIKO mice at 60 mg/kg once per day for 5 days. The same treatment also was applied to control Gpx4(f/f) mice.

The vitamin E deficient diet, an AIN-93G-modified rodent diet that lacks vitamin E, was formulated and manufactured by Bio-Serv (Flemington, NJ). To determine the effect of vitamin E deficiency on neurodegeneration, Gpx4BIKO mice and control Gpx4(f/f) mice were fed the vitamin E deficient diet starting at the age of 1 month. Tamoxifen was administered 6 weeks later to ablate Gpx4 in Gpx4BIKO mice.

Liproxstatin-1, a small-molecule ferroptosis inhibitor, was purchased from Selleckchem.com (Cat #-S7699). To evaluate the effect of ferroptosis inhibition on neurodegeneration, after being fed the vitamin E deficient diet for 6 weeks, Gpx4BIKO mice were treated with tamoxifen to ablate Gpx4, as described above. Two days into tamoxifen treatment, liproxstatin-1, which was dissolved in DMSO and then diluted in PBS, was given to one half of the mice via i.p. injection every two days at a dose of 10 mg/kg, whereas the other half of mice received i.p. injection of the vehicle (1.5% DMSO in PBS) only.

All animal procedures were reviewed and approved by the Institutional Animal Care and Use Committees of the University of Texas Health Science Center at San Antonio and the Audie Murphy Memorial Veterans Hospital, South Texas Veterans Health Care System.

2.2. Detection of cre-mediated Gpx4 ablation

A PCR-based method was used to detect Cre-mediated recombination of the floxed Gpx4 allele in genomic DNA isolated from tissues. PCR reactions were performed using primers (P1, 5′-TAC TGC AAC AGC TCC GAG TTC-3′; P2, 5′-CTT CAC CAC GCA GCC GTT CT-3′) that would produce a 700 bp-amplicon from the recombined Gpx4 (rGpx4) allele.

2.3. Behavior tasks

Spatial learning and memory function was assessed by the Morris Water Maze task as described [22]. In brief, mice were trained to find a hidden platform in opaque water for 5 days with 4 acquisition-trials per day from pseudorandomized start positions. Escape latency, or time to find the hidden platform, was recorded as an index of spatial learning and memory (60 s max). Probe trials (where the submerged platform was removed) were performed on day 6 after acquisition trials whereby total time spent searching in the area previously containing the platform was calculated as an additional memory metric (30 s max). Average acquisition-trial time (s) divided by distance traveled during that time (m) was calculated as a proxy for active participation in the task or what we call the motivational quotient (MQ). Significant deviations from the average MQ per group, declared as non-swimmers, were determined using the modified Thompsons tau technique for outlier detection and removed from the study. All Morris water maze trials were recorded and analyzed using the ANY-Maze tracking system (Stoelting, Chicago, IL).

Rotarod performance was evaluated using a Rotamex 4/8 (Columbus Instruments, Columbus, OH) machine following an accelerating rod protocol. The initial speed was set to 2 rpm with a linear acceleration to 40 rpm. Latency to fall was recorded as an index for locomotor ability at 4 trials per day with a 2–3 min inter-trial rest period.

2.4. Brain tissue section preparation and staining

Mice were anesthetized then transcardially perfused with PBS followed by 4% paraformaldehyde. Whole perfused brains were collected, post-fixed in 4% paraformaldehyde overnight at 4 °C, and then equilibrated in 30% sucrose in PBS for 3 days at 4 °C. Brains were sectioned at 16 μm using a cryostat (CM1850, Leica, Germany). For Nissl staining, sections were stained with 0.1% (w/v) cresyl violet for 5 min then dehydrated through graded ethanol rinses then cleared in xylene. Cresyl violet-stained sections were used to quantify cell number of the CA1 region of the hippocampus. Images were obtained with a 20× objective on a Zeiss Axio light microscope. Three different brain sections were quantified per mouse (n=3). Three CA1 region frames

were obtained per section and each frame contained three randomly selected, identical regions of interest (ROI; 2400 μm^2). The number of cells within each ROI was quantified with the cell counter tool of NIH ImageJ software and averaged per hippocampi.

For immunofluorescence staining, brain sections were re-hydrated in PBS for 10 min then placed in blocking buffer (10% BSA in PBS and 0.2% Triton X-100) for 1 h at room temperature. Sections were then incubated in blocking buffer containing primary antibody overnight at 4 °C. Slides were then washed 3 times in PBS followed by a 1 h incubation with secondary antibody conjugated to a fluorophore (ThermoFisher, MA). After washing 3 times, slides were mounted with DAPI containing ProLong Gold mounting media (ThermoFisher, MA). For Fluoro-Jade C (FJC) staining, sections were prepared as described [23] using 0.001% FJC solution (Millipore, MA) for 2 h and mounted with Acymount (StatLab, TX). Immunofluorescence and FJC images were obtained using an Olympus FV-1000 laser scanning confocal microscope (Olympus, PA). Three different brain sections per mouse were quantified. Three different CA1 region frames were collected with a 20× objective on a Zeiss Axio light microscope. Each frame contained three identical regions of interest (ROI; 1920.44 μm^2) with each containing an average of 12 cells. Images were converted from RGB to gray scale in order to quantify pixel intensity in NIH ImageJ software. Mean pixel intensity (mean gray value) per ROI was quantified with the Analyze/Measure tool of ImageJ software and then averaged per frame.

2.5. Antibodies and Western blotting

The following antibodies were used for this study: anti-NeuN (Millipore, MA); anti-synaptophysin, anti-GFAP, anti-β-Actin, anti-total ERK1/2, anti-phospho ERK1/2 (Cell Signaling, MA); anti-Iba-1 (Wako Chemicals USA, VA); anti-4-HNE (R & D Systems, Minneapolis, MN); anti-Gpx4 (in-house); anti-caspase-3 (Santa Cruz Biotechnology, CA); and anti-SNAP25 (AbCam, Cambridge, MA). Brain regions were dissected then homogenized in 1× RIPA buffer (20 mM Tris, pH7.4, 0.25 M NaCl, 1 mM EDTA, 0.5% NP-40, 50 mM sodium fluoride) with protease and phosphatase inhibitors (Roche, IN). In brief, 30 μg total protein per sample was separated by SDS-PAGE and transferred to PVDF membranes. Membranes were blocked with 5% BSA then incubated with primary antibody overnight at 4 °C. After incubation with fluorophore conjugated secondary antibodies (ThermoFisher, MA) for 1 h, bands were detected using an Odyssey scanner (LI-COR, Lincoln, NE). Signals were analyzed using NIH ImageJ software and normalized to that of β-Actin loading controls.

2.6. Real-Time qPCR

Total RNA was isolated with Trizol reagent (Sigma-Aldrich, St. Louis, MO) then reverse transcribed using the iScript RT kit (Bio-Rad, Hercules, CA). Real-Time qPCR was performed on the 7900HT platform (ThermoFisher, MA) using SYBR green chemistry (Bio-Rad, Hercules, CA). The mRNA levels were normalized to β-Actin to control for input RNA. Primers used were as follows: IL-6 (forward: 5′-CCG GAG AGG AGA CTT CAC AG-3′; reverse: TCC ACG ATT TCC CAG AGA AC-3′); TNF-α (forward, 5′-CTG AAC TTC GGG GTG ATC GG-3′; reverse, 5′- GGC TTG TCA CTC GAA TTT TGA GA-3′); GFAP (forward: 5′- GTT GGC AAC CTA TGG TTC GT -3′; reverse: 5′- CAG GAG CTG GTT GCT TTT CT –3′); Iba-1 (forward, 5′-ATC AAC AAG CAA TTC CTC GAT GA-3′; reverse, 5′-CAG CAT TCG CTT CAA GGA CAT A-3′); β-Actin (forward: 5′-ATC TGG CAC CAC ACC TTC TAC-3′; reverse: 5′-CAG GTC CAG ACG CAG GAT G-3′).

2.7. Statistical analysis

All data are expressed as mean ± SEM. Significant differences in Morris water maze and rotarod performances were calculated using repeated measures ANOVA for day (average of 4 trials) and genotype. Analysis was done using the XLSTAT package (Addinsoft, NY). *: $p < 0.05$ was considered significant for all analysis. Significance was assigned using Student's *t*-test for all other measures.

3. Results

3.1. Conditional ablation of Gpx4 in forebrain neurons of Gpx4BIKO mice

Lipid peroxidation, the driving force of ferroptosis, is associated with neurodegeneration in AD brains; however, whether ferroptosis is a modality of degeneration for those neurons remains unknown. We were interested in determining whether neurons in hippocampus and cortex regions are vulnerable to ferroptosis. To that end, we set out to generate a mouse model with conditional deletion of Gpx4, the key enzyme in detoxifying hydroperoxides in membrane lipids, in hippocampal and cortex neurons. We previously generated mice with floxed Gpx4 alleles: Gpx4(f/f) mice [20]. Camk2α-CreER(T2) transgenic mouse expresses a tamoxifen-activatable form of Cre recombinase in forebrain neurons [21]. So, we cross-bred Camk2α-CreER(T2) transgenic mice with Gpx4(f/f) mice, and produced mice with two floxed Gpx4 alleles and hemizygous for the Camk2α-CreER(T2) transgene [Gpx4(f/f);Camk2α-CreER(T2)$^{+/0}$]. We called them Gpx4 brain inducible knockout (Gpx4BIKO) mice.

We next tested the conditional ablation of Gpx4 in Gpx4BIKO mice. Gpx4BIKO mice (2–3 months of age) were treated with tamoxifen (TAM), and tissues from those mice were collected 2 weeks later for analysis. First, we used a PCR-based method to detect the recombined Gpx4 allele (rGpx4) in tissues from Gpx4BIKO mice (Fig. 1A). As Fig. 1B shows, rGpx4 was present in cerebral cortex and hippocampus tissues of TAM-treated Gpx4BIKO mice but not in spinal cord or liver tissues. Notably, rGpx4 was not detectable in cerebral cortex and hippocampus tissues from Gpx4BIKO mice without TAM treatment or in tissues from Gpx4(f/f) mice. We next compared levels of Gpx4 protein between TAM-treated Gpx4BIKO mice and control Gpx4(f/f) mice by Western blots. As Fig. 1C shows, TAM-treated Gpx4BIKO mice had a decreased level of Gpx4 protein in cortex and hippocampus tissues compared with control Gpx4(f/f) mice, and the decreased level of Gpx4 protein was maintained at 15 weeks after TAM treatment. We also looked at the neuronal level of Gpx4 by immunofluorescence. Brain sections from TAM-treated Gpx4BIKO mice and control mice were stained with the anti-Gpx4 antibody. As Fig. 1D shows, hippocampal neurons from TAM-treated Gpx4BIKO mice had a reduction of Gpx4 immunogenicity. Gpx4 plays a key role in reducing lipid hydroperoxides, thereby suppressing the generation of end-products of lipid peroxidation such as 4-hydroxynonenal (4-HNE). So, a loss of Gpx4 is predicted to increase 4-HNE level. Consistent with this prediction, an increased level of 4-HNE protein adducts was observed in cerebral cortex of TAM-treated-Gpx4BIKO mice (Fig. 1E). Taken together, these results indicate that TAM treatment induced a robust ablation of Gpx4 in forebrain neurons of Gpx4BIKO mice.

3.2. Gpx4 ablation resulted in cognitive impairment in Gpx4BIKO mice

We next examined how Gpx4 ablation might affect cognition of Gpx4BIKO mice. A cohort of Gpx4BIKO mice were treated with TAM at 2–3 months of age. Because preliminary data indicated that both TAM-treated Gpx4(f/f) mice and vehicle-treated Gpx4BIKO mice had normal cognitive function (data not shown), we chose to use TAM-treated Gpx4(f/f) mice (littermates of Gpx4BIKO mice) as controls so that we could efficiently use the mice that were produced. We assessed the cognitive function of TAM-treated Gpx4BIKO mice and TAM-treated Control mice by the Morris water maze task at week 6 after TAM treatment. As Fig. 2A shows, there was no statistically significant

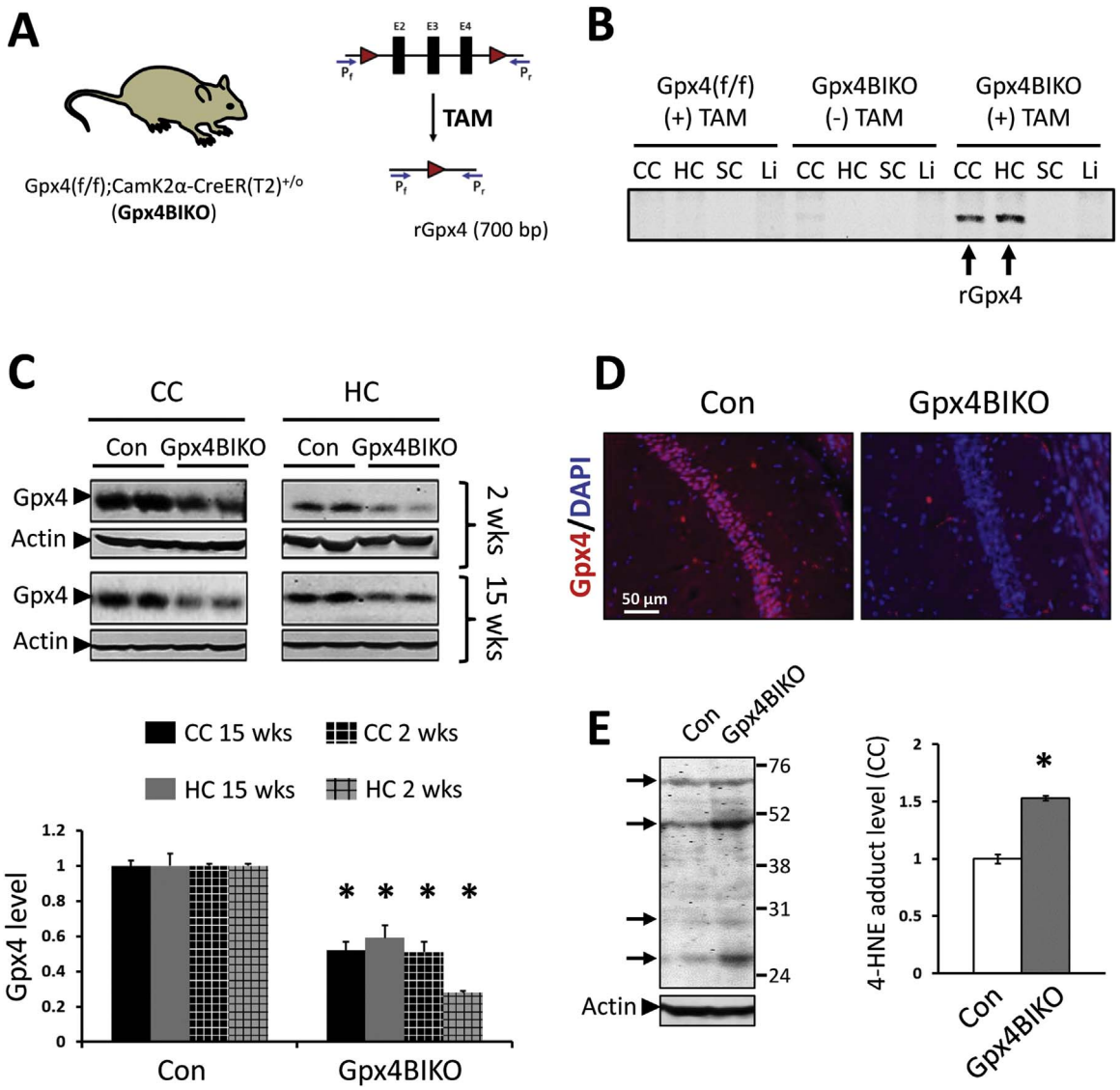

Fig. 1. Conditional ablation of Gpx4 in forebrain neurons of Gpx4BIKO mice. A. A scheme to ablate Gpx4 in forebrain neurons of mice with graphic of the Gpx4 allele showing loxP sites and primer sites to detect recombined Gpx4 (rGpx4) using PCR. B. A gel image of PCR results to detect rGpx4 in cerebral cortex (CC), hippocampus (HC), spinal cord (SC), and liver (Li) at 2 weeks post TAM treatment. C. Western blots showing decreased Gpx4 expression in CC and HC tissues in Gpx4BIKO at 2 weeks and 15 weeks post TAM treatment with quantification (below). D. Images of hippocampus (CA1 region) indicating reduced Gpx4 immunoreactivity in Gpx4BIKO mice at 2 weeks post TAM treatment. E. Western blot indicating elevated 4-HNE protein adducts in Gpx4BIKO mice at 2 weeks post TAM treatment with quantification. Arrows indicate bands with elevated signal at different protein sizes, and the numbers on the right are markers of Molecular Weight (kD). n=4–5 for all groups; $*p < 0.05$; Control animals (Con) were littermate Gpx4(f/f) mice.

difference in escape latencies between Gpx4BIKO and Control mice after 5 days of acquisition trials. We thought that 6 weeks might be too short of a time for Gpx4BIKO mice to develop cognitive impairment, so we decided to follow the mice longitudinally and re-tested their performance in Morris water maze task at week 12. As Fig. 2A and B shows, while Control mice exhibited normal spatial learning and memory function as indicated by their decreased escape latency associated with training, Gpx4BIKO mice showed no decrease in escape latency in this task. Further, after 5 days of acquisition trials, the difference in escape latencies between Gpx4BIKO mice and Control mice was statistically significant. We also compared the performance of Gpx4BIKO mice and Control mice in probe trials on day 6. As Fig. 2C shows, Gpx4BIKO mice spent significantly less time than Control mice in the target quadrant where the hidden platform was previously located. To ensure that the differences in Morris Water Maze performance by Gpx4BIKO mice was not confounded by locomotor deficit, we compared average swim speed between Gpx4BIKO mice and Control mice and saw no difference (Fig. 2D). We also assessed the locomotor function of Gpx4BIKO mice by a rotarod task. As Fig. 2E shows, no significant difference in rotarod performance was detected between the two groups, indicating that Gpx4BIKO mice had no compromised motor function. Taken together, these data indicate that ablation of Gpx4 in forebrain neurons induced cognitive impairment in Gpx4BIKO mice.

3.3. Degeneration of hippocampal neurons in cognitively impaired Gpx4BIKO mice

After completion of behavioral assessments, Gpx4BIKO and Control mice were sacrificed, and cerebral cortex and hippocampus tissues were collected from the mice. To determine whether cognitive impairment was associated with neurodegeneration in Gpx4BIKO mice, we compared levels of several neural proteins between Gpx4BIKO mice and Control mice by Western blots. The representative blots and quantified results are presented in Fig. 3A. While no differences in NeuN, synaptophysin and SNAP25 proteins were detected in cerebral cortex tissues from the two groups, compared with Control mice, Gpx4BIKO mice exhibited decreased levels of those

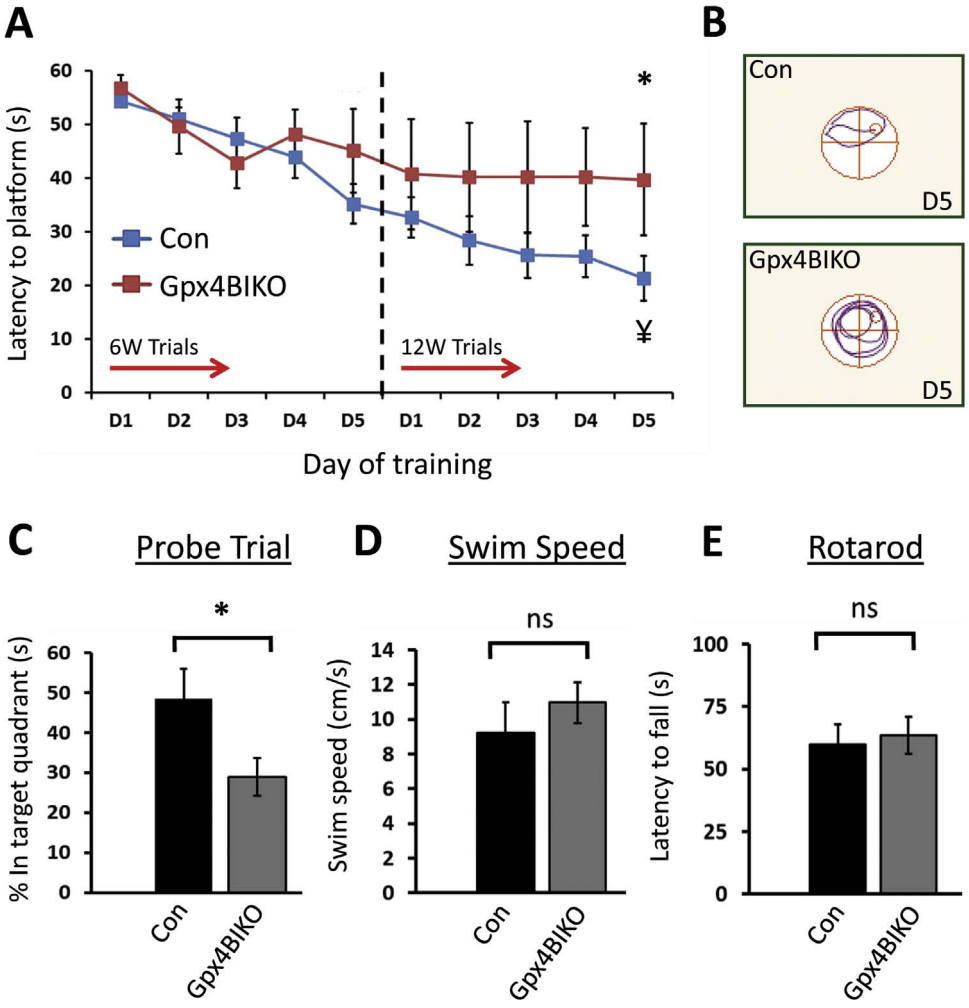

Fig. 2. Impaired spatial learning and memory abilities in Gpx4BIKO mice. A. Escape latencies of Gpx4BIKO and Control (Con) mice in Morris water maze (MWM) task at 6 and 12 weeks post TAM treatment, respectively. B. Representative MWM swim plots for Gpx4BIKO and Con mice from day 5 of the 12-week MWM task. C. Percent time spent in the target quadrant in probe trials on day 6 of the 12-week MWM task. D. No difference in average swim speed between Gpx4BIKO and Control mice (collected from day 5 of acquisition trials). E. Rotarod performance of Gpx4BIKO and Con mice assessed after completion of the 12-week MWM task. Data shown are latencies to fall (average of 4 trials) after 1 day of training to acclimate the mice to the task. For all behavior tasks, n=15 for Gpx4BIKO mice, n=8 for Control mice (f/f). $^{*}p < 0\ 0.05$ for Gpx4BIKO versus Control for same day performance; $^{¥}p < 0.05$ for Control mice at start of water maze testing versus control mice on the final day of water maze testing indicating learning; ns, the difference is not statistically significant.

neural proteins in hippocampus tissues, suggesting degeneration of hippocampal neurons. To corroborate the results of the Western blots, we analyzed hippocampus region of Gpx4BIKO mice by histology. The Nissl-stained images of hippocampus regions and quantified numbers of CA1 neurons of Gpx4BIKO mice and Control mice are presented in Fig. 3B. From those results, it is evident that Gpx4BIKO mice had a significant loss of neurons in the CA1 layer of the hippocampus. Fluoro-Jade C is a fluorescent stain that reacts specifically with degenerating or "injured" neurons [23]. To assess the health status of remaining hippocampal neurons of Gpx4BIKO mice, we measured their reactivity to Fluoro-Jade C. As Fig. 3C shows, Fluoro-Jade C reactivity of CA1 neurons of Gpx4BIKO mice was significantly increased compared with that of Control mice. The results of hippocampal neuron degeneration were consistent with the impaired spatial learning and memory function (a hippocampus dependent cognitive task) observed in those mice. The finding that neurodegeneration in Gpx4BIKO mice occurred in hippocampus is also consistent with other reports showing the increased sensitivity of hippocampal neurons, particularly the pyramidal neurons in the CA1 layer, to oxidative stress [24].

3.4. Ferroptotic features associated with neurodegeneration in Gpx4BIKO mice

Gpx4 is a key regulator of ferroptosis [17]. With this in mind, we wondered whether neurodegeneration observed in Gpx4BIKO mice occurred through ferroptosis. Although no specific markers of ferroptosis have been identified, several features in combination separate ferroptotic cell death from apoptotic cell death [25]. Because lipid peroxidation is the driving force of ferroptosis, cells dying through ferroptosis are expected to have an elevated level of lipid peroxidation. So we assessed the status of lipid peroxidation in the cognitively impaired Gpx4BIKO mice by Western blots against 4-HNE protein adducts. As the results in Fig. 4A show, Gpx4BIKO mice exhibited a significantly elevated level of 4-HNE adducts in hippocampal and cortical proteins compared with Controls, indicating increased lipid peroxidation. Activation of ERK is also associated with ferroptosis [26], so we next determined the level of ERK1/2 phosphorylation in Gpx4BIKO mice. Compared to Controls, Gpx4BIKO mice showed elevated ERK1/2 phosphorylation in both hippocampus and cerebral cortex tissues (Fig. 4B). Ferroptosis is also independent of caspase-3 activation, a classical marker of apoptotic cell death. To determine whether activation of caspase-3 occurred in Gpx4BIKO mice, we tried to detect cleaved caspase-3 (the activated form of caspase-3) by

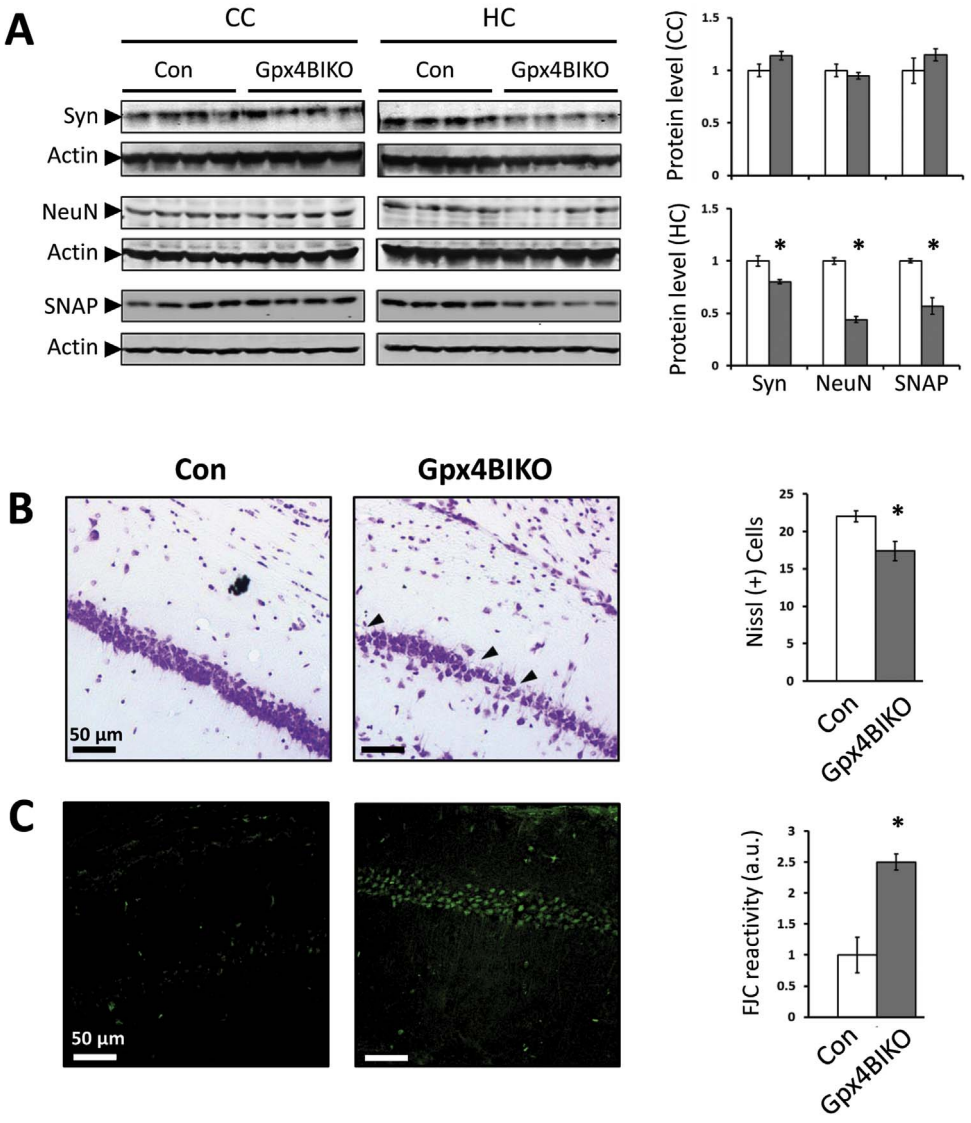

Fig. 3. Hippocampal neurodegeneration in cognitively impaired Gpx4BIKO mice. A. Western blots showing levels of neural proteins synaptophysin (Syn), synaptosome associated protein-25 (SNAP), and NeuN, in cerebral cortex (CC) and hippocampus (HC) tissues of Gpx4BIKO mice with quantification (right), n=5. B. Nissl stained HC sections indicating neuronal loss in CA1 region (black arrows) in Gpx4BIKO mice with quantification representing average number of Nissl positive cells, n=3. C. Images of Fluoro-Jade C stained HC sections indicating degenerating CA1 neurons in Gpx4BIKO mice with quantification, n=3. * $p < 0.05$; Control animals were Gpx4(f/f); tissues were collected after completion of behavioral tasks at 15 weeks post TAM treatment.

Western blots. As Fig. 4C shows, we did not observe any cleaved caspase-3 in hippocampus or cortex tissues of Gpx4BIKO mice. Cells dying through ferroptosis but not apoptosis can trigger inflammation by releasing damage-associated molecular patterns (DAMPs) and immunogenic lipid metabolites [12,13]. So, we further assessed the status of inflammation in brains of Gpx4BIKO mice. We first compared microgliosis and astrogliosis by determining levels of the most common glial markers, Iba-1 for microglia and GFAP for astrocytes, by Western blots. As Fig. 5A shows, compared with Control mice, Gpx4BIKO mice had significantly elevated levels of Iba-1 and GFAP proteins. To corroborate the Western blot results, we next compared levels of microgliosis and astrogliosis between the two groups by immunofluorescence. The confocal microscopy images of hippocampus regions are shown in Fig. 5B. Compared with Control mice, significantly elevated immunofluorescence signals for both Iba-1 and GFAP were present in the CA1 region of hippocampus in Gpx4BIKO mice. Interestingly, microglia in particular appeared to infiltrate the pyramidal neurons of the CA1 layer where degeneration was the most overt (Fig. 5B). Reactive or activated astrocytes and microglia potentiate neuroinflammation through the production of pro-inflammatory cytokines such as TNF-α and IL-6. So, we also compared levels of TNFα and IL-6 as well as levels of Iba-1 and GFAP by Real-Time quantitative PCR. As expected, Gpx4BIKO animals showed up-regulated transcript levels of cytokines IL-6 and TNF-α, in addition to that of Iba-1 and GFAP (Fig. 5C). The increased lipid peroxidation, ERK activation, lack of cleaved caspase-3 and in particular the overt neuroinflammation, suggested that ferroptosis but not apoptosis was likely responsible for the observed hippocampal neurodegeneration in Gpx4BIKO mice.

3.5. A deficiency of Vitamin E, an antioxidant with ferroptosis inhibition activity, expedited neurodegeneration in Gpx4BIKO mice

We next asked whether neurodegeneration in Gpx4BIKO mice could be altered by manipulations that affect the anti-ferroptosis defense system. Vitamin E (α-tocopherol) is a lipid soluble antioxidant that exhibits ferroptosis inhibition activity [11]. So we were interested in determining how a deficiency of vitamin E might affect Gpx4BIKO mice. To that end, we placed Gpx4BIKO mice and Control mice on a

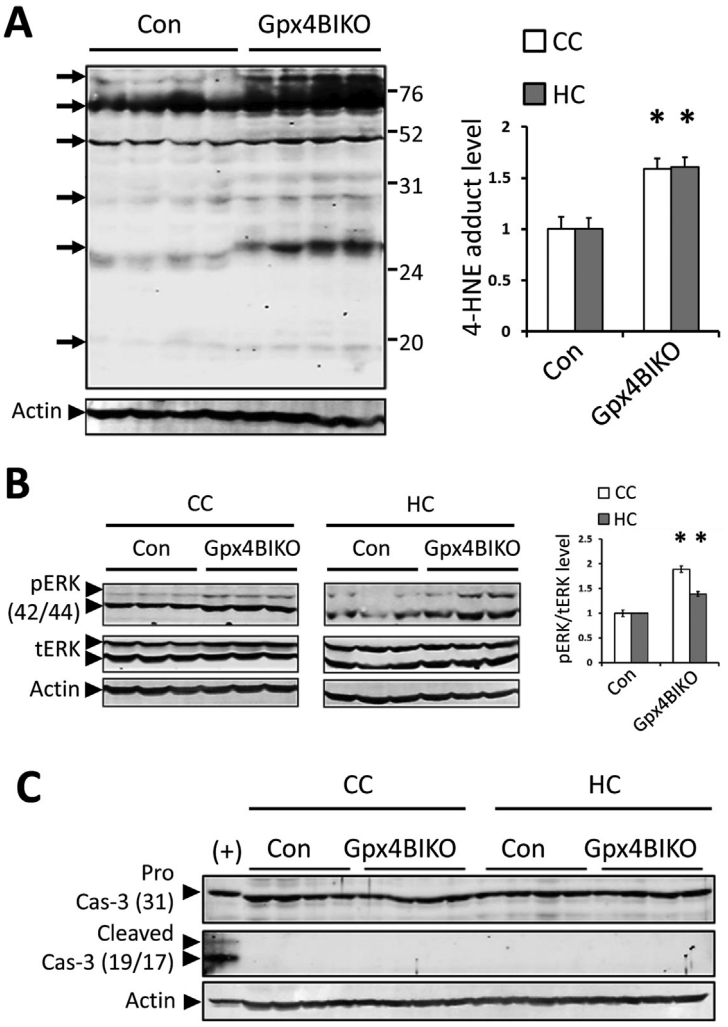

Fig. 4. Signatures of ferroptosis in cognitively impaired Gpx4BIKO mice. A. Western blot of 4-HNE adduct levels from cerebral cortex (CC) tissue (hippocampus (HC) blot not shown) with quantification for CC and HC. Arrows indicate bands with elevated signal at different protein sizes, and the numbers on the right are markers of Molecular Weight (kD). B. Western blots detecting phosphorylated (activated) ERK(1/2) and total ERK(1/2) in CC and HC tissues of Gpx4BIKO mice versus controls. pERK(1/2) levels were quantified relative to total ERK(1/2) expression levels. C. Western blot showing procaspase-3 and lack of cleaved (activated) caspase-3 in CC or HC in Gpx4BIKO animals versus controls. (+) control was cytochrome C-treated jurkat cell extracts (Cell Signaling, Inc.). n=5 for all groups; $^{*}p < 0.05$; Control animals were Gpx4(f/f).

vitamin E deficient diet for 6 weeks prior to treatment with TAM. Strikingly, after TAM treatment, Gpx4BIKO mice fed the vitamin E deficient diet (Gpx4BIKO-VED) exhibited an ataxia-like, hindlimb clasping behavior, suggesting locomotor dysfunction (Fig. 6A). We therefor further assessed the locomotor function of mice by the rotarod task. As Fig. 6A shows, compared with Control mice (Con-VED), Gpx4BIKO-VED mice had a significant decreased rotarod performance, confirming locomotor dysfunction. Locomotor dysfunction of Gpx4BIKO-VED mice could arise from abnormalities of neuron populations in several brain regions; however, for this study, we were only interested in determining how feeding the vitamin E deficient diet might affect hippocampal neurodegeneration in Gpx4BIKO mice. To that end, we collected hippocampus tissues from the mice at 1 week after TAM treatment, and compared levels of NeuN, synaptophysin and SNAP25 by Western blots. As the results in Fig. 6B show, Gpx4BIKO-VED mice had significant lower levels of those neural proteins than Con-VED mice. Because Gpx4BIKO mice on the standard chow diet didn't show neurodegeneration in hippocampus until about 15 weeks after TAM treatment, those results thus indicate that a deficiency of vitamin E exacerbated hippocampal neurodegeneration in Gpx4BIKO mice. Aside from the expedited neurodegeneration, Gpx4BIKO-VED mice also had significantly higher levels of GFAP and Iab-1 at 1 week after TAM treatment than Con-VED mice, indicating augmented brain inflammation (Fig. 6B).

3.6. Neurodegeneration in Gpx4BIKO mice fed the vitamin E deficient diet was ameliorated by ferroptosis inhibitor liproxstatin-1

The results that vitamin E deficiency expedited neurodegeneration and inflammation further suggested ferroptosis was a mechanism of neurodegeneration in Gpx4BIKO mice. At present, no specific markers of ferroptosis have been established that allow ferroptosis to be conveniently differentiated from apoptosis or other programmed cell death mechanisms. At cellular level, ferroptosis is best-characterized as a mode of cell death induced by compounds such as erastin, BSO, RSL3, etc. and inhibited by compounds such as ferrostatin-1, trolox, liproxstatin-1, 16-86, etc. [11–13,17]. Liproxstatin-1 is a small-molecule compound that exhibits specific inhibition activity of ferroptosis both in vitro and in vivo [13]. So we evaluated the effects of liproxstatin-1 on Gpx4BIKO-VED mice. Liproxstatin-1 was administered to Gpx4BIKO mice at a dose of 10 mg/kg every 2 days beginning at day 1 of TAM treatment. Effects of liproxstatin-1 treatment in Gpx4BIKO-VED mice were compared against Gpx4BIKO-VED mice treated with vehicle (DMSO) or Gpx4(f/f) animals on the VED diet (Con-VED). Knowing that locomotor dysfunction started to appear in Gpx4BIKO mice within a few days following TAM treatment, we first

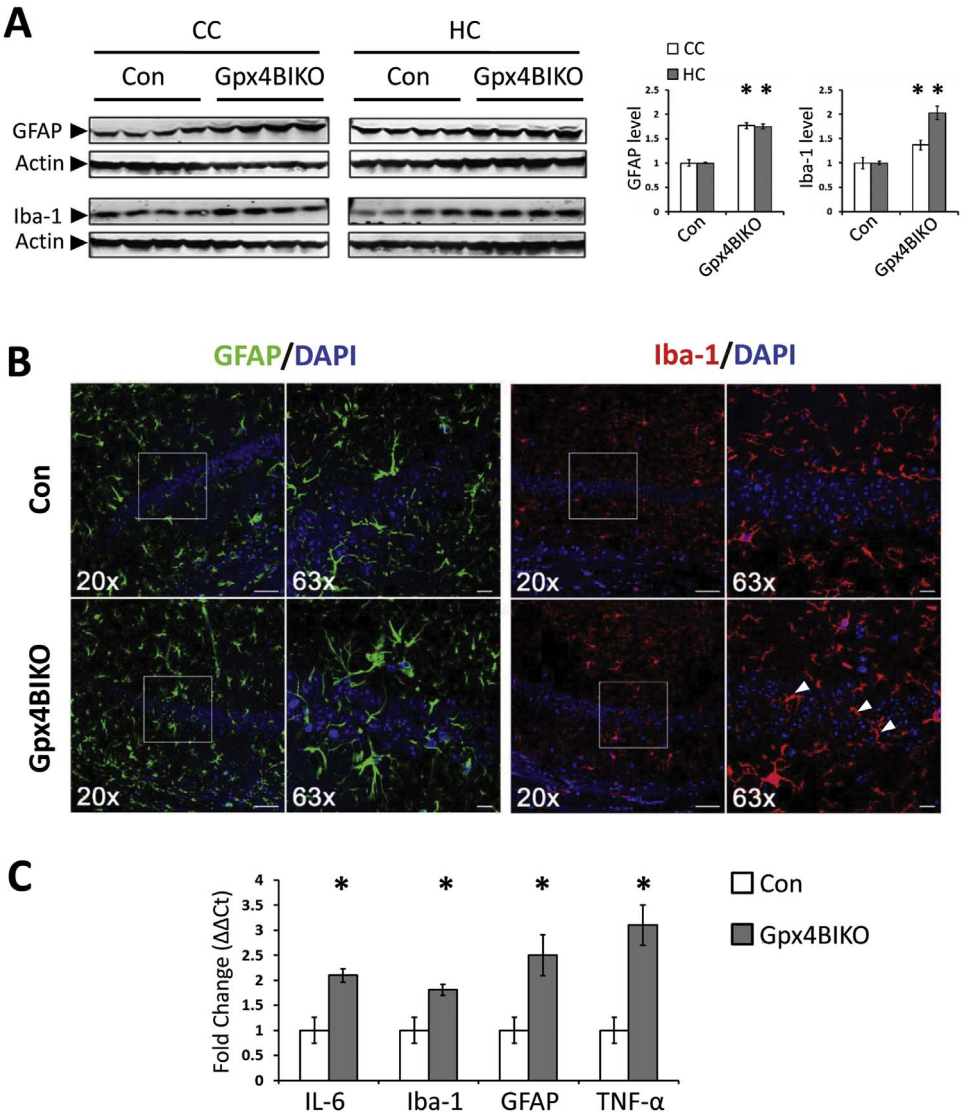

Fig. 5. Neuroinflammation in cognitively impaired Gpx4BIKO mice. A. Western blots showing expression of astrogliosis marker (GFAP) and microgliosis marker (Iba-1) in cerebral cortex (CC) and hippocampus (HC) tissues of Gpx4BIKO mice with quantification (right), n=5. B. Immunofluorescent images indicating gliosis markers GFAP (green) and Iba-1 (red) in the CA1 region of the hippocampus at 20X and 63X with DAPI (blue). White arrows indicate microglia infiltration of CA1 pyramidal neuron layer. C. Relative mRNA expression of proinflammatory cytokines (IL-6, TNF-α) and gliosis markers (GFAP, Iba-1) in CC tissue using Real-Time qPCR, n=4. $*p < 0.05$; Control animals were Gpx4(f/f) mice. (For interpretation of the references to color in this figure legend, the reader is referred to the web version of this article).

measured rotarod performance for the three groups starting at day 1 of TAM treatment. Gpx4BIKO-VED mice treated with liproxstatin-1 showed a consistently higher, but not significant rotarod performance (n=6, p=0.076) versus DMSO-treated Gpx4BIKO-VED mice suggesting a subtle behavioral rescue (data not shown). We next collected hippocampus tissues from those mice at 1 week post TAM treatment and compared the levels of neural marker proteins. As Fig. 6C shows, Gpx4BIKO-VED mice treated with liproxstatin-1 had higher levels of neural protein NeuN, Synaptophysin, and SNAP25 than Gpx4BIKO-VED mice treated vehicle. In fact, the levels of the three neural proteins in Gpx4BIKO-VED mice were similar to that of Con-VED mice (Fig. 6C). In addition, Gpx4BIKO-VED mice treated with liproxstatin-1 also exhibited a decreased level of the astrogliosis marker GFAP versus Gpx4BIKO-VED mice treated with vehicle. Overall, the results of liproxstatin-1 attenuating hippocampal neurodegeneration and inflammation in Gpx4BIKO-VED mice further highlight ferroptosis as a major contributor of neurodegeneration in Gpx4BIKO mice.

4. Discussion

The brain is vulnerable to increased ROS because of its high metabolic rate and relatively low antioxidant defense capability. Oxidative damage in the brain predominantly manifests as lipid peroxidation due to the high concentration of PUFAs present in its membrane rich architecture [27]. Lipid peroxidation can significantly disrupt cellular function, and a high level of which is the driving force of ferroptosis [15]. Gpx4 can suppress lipid peroxidation by directly reducing hydroperoxides in membrane lipids, and is shown to regulate ferroptotic cell death [17]. In this study, we assessed whether Gpx4 ablation could elicit degeneration of forebrain neurons (cerebral cortex and hippocampus). After TAM treatment to ablate Gpx4, Gpx4BIKO mice developed impairment in hippocampus dependent spatial learning and memory function. Cognitive impairment in Gpx4BIKO mice also was associated with hippocampal neurodegeneration most prominently in the CA1 layer. Consistent with the role of Gpx4 as a key regulator of ferroptosis, we found that cognitive impairment and neurodegeneration in Gpx4BIKO mice was associated with elevated lipid peroxidation, ERK(1/2) activation, and overt neuroinflammation

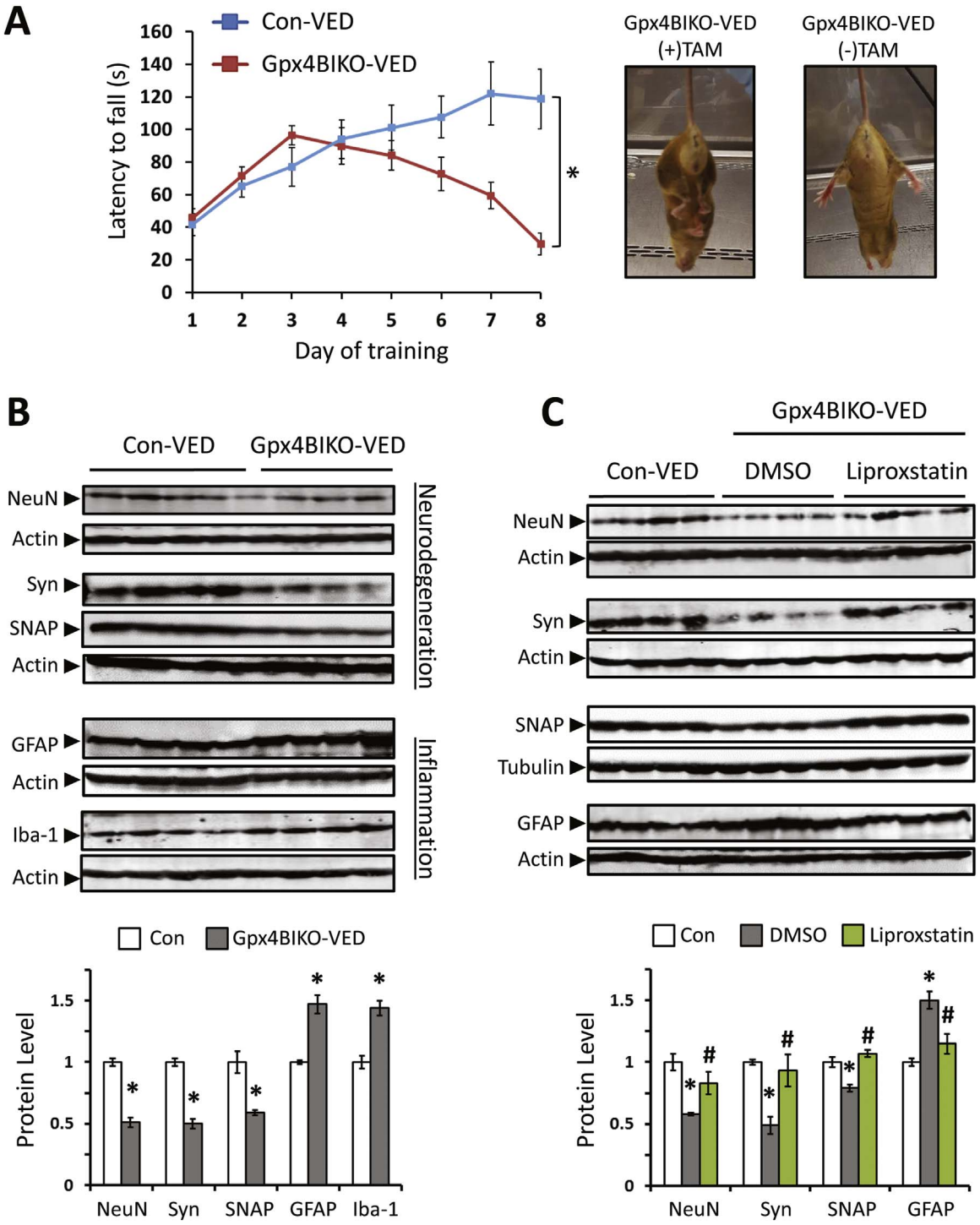

Fig. 6. Exacerbated neurodegeneration in Gpx4BIKO mice fed a vitamin E deficient diet. A. Rotarod performance for Gpx4BIKO mice and Control mice that were fed a vitamin E deficient diet after TAM treatment beginning on day 1 (n=6 for both groups). Image of Gpx4BIKO mice fed the vitamin E deficient diet (Gpx4BIKO-VED) demonstrating a hindlimb clasping phenotype at 1 week post TAM treatment. B. Western blots showing reduced levels of neural proteins NeuN, Synaptophysin, and SNAP25 as well as elevated levels of gliosis markers GFAP and Iba-1 at 1 week post TAM treatment in Gpx4BIKO-VED mice (n=5 for both groups). C. Western blots showing attenuated neurodegeneration (NeuN, Synaptophysin, SNAP25) and neuroinflammation (GFAP) in HC of Gpx4BIKO-VED mice treated with the ferroptosis inhibitor liproxstatin-1 compared to Gpx4BIKO-VED mice treated with vehicle (DMSO) at 1 week post TAM treatment (n=5 for all groups). * $p < 0.05$ versus Con-VED; $^{\#}p < 0.05$ versus Gpx4BIKO-VED treated with DMSO.

with no detectable caspase-3 activation which are all indicative of ferroptotic but not apoptotic cell death. In addition, removal of vitamin E, an inhibitor of ferroptosis, from the diet of Gpx4BIKO mice for 6 weeks prior to TAM treatment lead to compromised locomotor ability. Importantly, hippocampal neurodegeneration was expedited in Gpx4BIKO mice fed the vitamin E deficient diet, appearing at 1 week after TAM treatment while neurodegeneration was not noticed until about 15 weeks after TAM treatment in Gpx4BIKO mice on a normal chow diet. In addition, using the ferroptosis inhibitor liproxstatin-1, we were able to mitigate neurodegeneration and inflammation observed in the Gpx4BIKO. Overall, those results strongly implicated ferroptosis and not apoptosis as the mechanism driving neurodegeneration in Gpx4BIKO mice.

Although the link between lipid peroxidation and neurodegenera-

tive diseases has long been known, the discrete contributions of lipid peroxidation stress that promote neurodegeneration are poorly understood. Here, we present another potential means by which lipid peroxidation stress in neurons may promote hippocampal neurodegeneration and cognitive impairment through ferroptotic cell death. Although ferroptosis was initially identified as a non-apoptotic cell death in oncogenic HRAS-containing cancer cell lines [26], subsequent studies indicate that ferroptosis is a mode of cell death in ischemic injury [12]. Importantly, ferroptosis may be a key mode of cell death in neurodegeneration. For example, ferroptosis is implicated in excitotoxicity-induced neuron death [11]. Do and colleagues showed that ferroptosis is also involved in death of midbrain neurons in Parkinson's disease [28]. Our previous study indicated that ferroptosis appeared to be a key mechanism of spinal motor neuron degeneration [19]. In this proof-of-concept study, we showed that forebrain neurons, which are severely afflicted in AD patients, are also vulnerable to ferroptosis. Although the precise contributions of ferroptosis in pathogenesis of various neurodegenerative diseases remain to be illustrated, a key question for future research is to determine whether ferroptosis could serve as a target of intervention for diseases such as AD. For example, Gpx4 has been implicated in neural protection [29,30] and could potentially present a target for therapeutic intervention. Moreover, many small-molecule inhibitors of ferroptosis are being identified and generated [31] with potential neuroprotective abilities by curbing neurodegeneration and downstream cognitive decline.

The ability to induce neuronal cell loss through conditional Gpx4 ablation, and exaggerate it by vitamin E deprivation, nicely illustrates the specific effects of lipid peroxidation in neurons in the context of neurodegeneration and cognitive impairment. It is particularly intriguing to us that three pronounced hallmarks of ferroptosis, (iron dysregulation, lipid peroxidation, inflammation) are also significant prodromal indices of AD and related dementias. Thus, ferroptosis could reflect an unappreciated pathological player in the context of neurodegenerative dementias like AD.

Author contributions

Q.R. and W.S.H. designed the experiments. W.S.H., R.S.F., L.C., and R.N. conducted experiments. Q.R. and W.S.H. wrote the manuscript.

Conflict of interest

The authors declare no conflicts of interest.

Acknowledgements

Q.R. is supported by a Merit Review Grant (I01BX1382) from Department of Veteran Affairs, and a Grant (IIRG-12-242388) from Alzheimer's Association.

References

[1] C.W. Cotman, A.J. Anderson, A potential role for apoptosis in neurodegeneration and Alzheimer's disease, Mol. Neurobiol. 10 (1) (1995) 19–45.
[2] M.P. Mattson, Neuronal life-and-death signaling, apoptosis, and neurodegenerative disorders, Antioxid. Redox Signal. 8 (11–12) (2006) 1997–2006.
[3] P.J. Khandelwal, A.M. Herman, C.E. Moussa, Inflammation in the early stages of neurodegenerative pathology, J. Neuroimmunol. 238 (1–2) (2011) 1–11.
[4] X. Wang, W. Wang, L. Li, G. Perry, H.G. Lee, X. Zhu, Oxidative stress and mitochondrial dysfunction in Alzheimer's disease, Biochim. Biophys. Acta (2013).
[5] P.H. Gordon, D.H. Moore, R.G. Miller, J.M. Florence, J.L. Verheijde, C. Doorish, J.F. Hilton, G.M. Spitalny, R.B. MacArthur, H. Mitsumoto, et al., Efficacy of minocycline in patients with amyotrophic lateral sclerosis: a phase III randomised trial, Lancet Neurol. 6 (12) (2007) 1045–1053.
[6] PRECEPT investigators of the Parkinson's Study Group, Mixed lineage kinase inhibitor CEP-1347 fails to delay disability in early Parkinson disease, Neurology 69 (15) (2007) 1480–1490.
[7] W.R. Markesbery, J.M. Carney, Oxidative alterations in Alzheimer's disease, Brain Pathol. 9 (1) (1999) 133–146.
[8] D.A. Butterfield, C.M. Lauderback, Lipid peroxidation and protein oxidation in Alzheimer's disease brain: potential causes and consequences involving amyloid beta-peptide-associated free radical oxidative stress, Free Radic. Biol. Med. 32 (11) (2002) 1050–1060.
[9] D. Pratico, S. Sung, Lipid peroxidation and oxidative imbalance: early functional events in Alzheimer's disease, J. Alzheimers Dis. 6 (2) (2004) 171–175.
[10] R.J. Castellani, P.I. Moreira, G. Liu, J. Dobson, G. Perry, M.A. Smith, X. Zhu, Iron: the redox-active center of oxidative stress in Alzheimer disease, Neurochem. Res. 32 (10) (2007) 1640–1645.
[11] S.J. Dixon, K.M. Lemberg, M.R. Lamprecht, R. Skouta, E.M. Zaitsev, C.E. Gleason, D.N. Patel, A.J. Bauer, A.M. Cantley, W.S. Yang, et al., Ferroptosis: an iron-dependent form of nonapoptotic cell death, Cell 149 (5) (2012) 1060–1072.
[12] A. Linkermann, R. Skouta, N. Himmerkus, S.R. Mulay, C. Dewitz, Z.F. De, A. Prokai, G. Zuchtriegel, F. Krombach, P.S. Welz, et al., Synchronized renal tubular cell death involves ferroptosis, Proc. Natl. Acad. Sci. USA 111 (2014) 16836–16841.
[13] J.P. Friedmann Angeli, M. Schneider, B. Proneth, Y.Y. Tyurina, V.A. Tyurin, V.J. Hammond, N. Herbach, M. Aichler, A. Walch, E. Eggenhofer, et al., Inactivation of the ferroptosis regulator Gpx4 triggers acute renal failure in mice, Nat. Cell Biol. 16 (12) (2014) 1180–1191.
[14] M.T. Heneka, M.K. O'Banion, D. Terwel, M.P. Kummer, Neuroinflammatory processes in Alzheimer's disease, J. Neural Transm. 117 (8) (2010) 919–947.
[15] W.S. Yang, B.R. Stockwell, Ferroptosis: death by lipid peroxidation, Trends Cell Biol. 26 (3) (2016) 165–176.
[16] A.W. Girotti, Lipid hydroperoxide generation, turnover, and effector action in biological systems, J. Lipid Res. 39 (8) (1998) 1529–1542.
[17] W.S. Yang, R. SriRamaratnam, M.E. Welsch, K. Shimada, R. Skouta, V.S. Viswanathan, J.H. Cheah, P.A. Clemons, A.F. Shamji, C.B. Clish, et al., Regulation of ferroptotic cancer cell death by GPX4, Cell 156 (1–2) (2014) 317–331.
[18] M. Matsushita, S. Freigang, C. Schneider, M. Conrad, G.W. Bornkamm, M. Kopf, T cell lipid peroxidation induces ferroptosis and prevents immunity to infection, J. Exp. Med. 212 (4) (2015) 555–568.
[19] L. Chen, W.S. Hambright, R. Na, Q. Ran, Ablation of the ferroptosis inhibitor glutathione peroxidase 4 in neurons results in rapid motor neuron degeneration and paralysis, J. Biol. Chem. 290 (47) (2015) 28097–28106.
[20] S.E. Yoo, L. Chen, R. Na, Y. Liu, C. Rios, R.H. Van, A. Richardson, Q. Ran, Gpx4 ablation in adult mice results in a lethal phenotype accompanied by neuronal loss in brain, Free Radic. Biol. Med. 52 (9) (2012) 1820–1827.
[21] L. Madisen, T.A. Zwingman, S.M. Sunkin, S.W. Oh, H.A. Zariwala, H. Gu, L.L. Ng, R.D. Palmiter, M.J. Hawrylycz, A.R. Jones, et al., A robust and high-throughput cre reporting and characterization system for the whole mouse brain, Nat. Neurosci. 13 (1) (2010) 133–140.
[22] L. Chen, R. Na, E. Boldt, Q. Ran, NLRP3 inflammasome activation by mitochondrial reactive oxygen species plays a key role in long-term cognitive impairment induced by paraquat exposure, Neurobiol. Aging 36 (9) (2015) 2533–2543.
[23] L.C. Schmued, C. Albertson, W. Slikker Jr., Fluoro-Jade: a novel fluorochrome for the sensitive and reliable histochemical localization of neuronal degeneration, Brain Res. 751 (1) (1997) 37–46.
[24] X. Wang, E.K. Michaelis, Selective neuronal vulnerability to oxidative stress in the brain, Front. Aging Neurosci. 2 (2010) 12.
[25] Y. Xie, W. Hou, X. Song, Y. Yu, J. Huang, X. Sun, R. Kang, D. Tang, Ferroptosis: process and function, Cell Death Differ. 23 (3) (2016) 369–379.
[26] N. Yagoda, R.M. von, E. Zaganjor, A.J. Bauer, W.S. Yang, D.J. Fridman, A.J. Wolpaw, I. Smukste, J.M. Peltier, J.J. Boniface, et al., RAS-RAF-MEK-dependent oxidative cell death involving voltage-dependent anion channels, Nature 447 (7146) (2007) 864–868.
[27] J.T. Coyle, P. Puttfarcken, Oxidative stress, glutamate, and neurodegenerative disorders, Science 262 (5134) (1993) 689–695.
[28] V.B. Do, F. Gouel, A. Jonneaux, K. Timmerman, P. Gele, M. Petrault, M. Bastide, C. Laloux, C. Moreau, R. Bordet, et al., Ferroptosis, a newly characterized form of cell death in Parkinson's disease that is regulated by PKC, Neurobiol. Dis. (2016).
[29] Q. Ran, M. Gu, H. Van Remmen, R. Strong, J.L. Roberts, A. Richardson, Glutathione peroxidase 4 protects cortical neurons from oxidative injury and amyloid toxicity, J. Neurosci. Res. 84 (1) (2006) 202–208.
[30] M.H. Yoo, X. Gu, X.M. Xu, J.Y. Kim, B.A. Carlson, A.D. Patterson, H. Cai, V.N. Gladyshev, D.L. Hatfield, Delineating the role of glutathione peroxidase 4 in protecting cells against lipid hydroperoxide damage and in Alzheimer's disease, Antioxid. Redox Signal. 12 (7) (2010) 819–827.
[31] S. Hofmans, T. Vanden Berghe, L. Devisscher, B. Hassannia, S. Lyssens, J. Joossens, P. Van Der Veken, P. Vandenabeele, K. Augustyns, Novel ferroptosis inhibitors with improved potency and ADME properties, J. Med. Chem. 59 (5) (2016) 2041–2053.